Analytical Electron Microscopy discloses Actual Structure of Zinc–Graphite *

Alois Fürstner and Hans Weidmann
Institute of Organic Chemistry, Technical University, Stremayrgasse 16, A-8010 Graz, Austria
Ferdinand Hofer
Institute for Electron Microscopy and Fine Structure Research, Steyrergasse 17, A-8010 Graz, Austria

Contrary to previous assumptions zinc–graphite obtained by the reduction of zinc chloride with lamellar potassium–graphite (C_8K) consists of finely dispersed zinc unevenly distributed on graphite as a support. While combined energy-dispersive *X*-ray analysis spectroscopy, electron energy loss spectroscopy, electron and *X*-ray diffraction showed no sign of intercalation of zinc in the graphite lattice it clearly proved the deleterious effect of water on the highly active metals. In fact, water-treated zinc–graphite is completely converted to zinc oxide on graphite.

The efficiency of chemical reactions involving metals as catalysts or reducing agents for various transformations largely depends on the active surface area,[1] which is generally a direct function of the degree of metal dispersion. Because of its importance the continuous interest in metal activation[2] has led to a respectable variety of activating procedures, such as simple grinding, dispersion to blacks and colloids,[3] formation of amalgams[4] and metal couples,[5,6] ultrasonic irradiation,[7] co-condensation with an inert solvent,[8] reduction of metal salts in solution,[9] and, last but not least, fine dispersion on various supports.[10,11] It was the method of metal salt reduction by lamellar potassium–graphite (C_8K)[11] that has recently led to considerable scope to extend the chemistry of zinc[5,12,13] and magnesium[14] and that is presently about to become the chosen activating procedure for the various metal-induced reductions.[11–14] However, despite good evidence for the existence of metal–graphite intercalation products,[15] a lamellar structure for *e.g.* zinc–graphite,[16,17] obtained from zinc chloride by C_8K reduction, appeared rather doubtful.[13] Not only must the treatment of zinc–graphite with water[13,16] be quite deleterious to the finely dispersed zinc, but in addition mere *X*-ray diffraction is an inadequate technique inasmuch as it provides structural information of large sample areas only.[18,19] Particle sizes below *ca.* 0.1 μm are invariably beyond the scope of this method.

For the conclusive elucidation of detailed structures of metal–graphite compounds, a prerequisite for the understanding of the relation between morphology and activity, an investigation by analytical electron microscopy (a.e.m.)[20,21] and electron diffraction of discrete areas of unimpaired samples supplemented by *X*-ray diffraction was called for. This combination of techniques offers the advantages of (*i*) detection of particle sizes well below 10 nm, (*ii*) chemical characterization of single phases in small specimen areas of a few nanometres by energy-dispersive *X*-ray (e.d.x.) spectrometry and/or electron energy loss spectroscopy (e.e.l.s.), and (*iii*) crystallographic analysis of microstructures and of structural relationships between different phases by *X*-ray and electron diffraction techniques.

Experimental

Preparation of Zinc–Graphite.—Samples were invariably prepared by rapid addition of freshly fused $ZnCl_2$ (7.5 mmol) in three equal portions to a stirred suspension of C_8K †,[5,11,12] (15 mmol) in anhydrous tetrahydrofuran (thf) (30 cm^3) under a stream of argon at room temperature causing the solvent to boil. After 30 min at reflux the black suspension was cooled and immediately subjected to instrumental analysis.

For a comparative investigation a sample of equal quantity was filtered, taking precautions to avoid self-ignition, washed with a sufficient amount of water to completely remove KCl, and finally washed with three portions (each 30 cm^3) of thf.

Analytical Electron Microscopy and X-*Ray Diffraction Analysis.*—Depending on the respective technique employed [e.d.x., e.e.l.s., or selected area electron diffraction (s.a.e.d.)] in each case part of the suspension was quickly dispersed on either $(SiO)_n$ or amorphous carbon thin film, each mounted on a nickel grid.

The Philips EM 420 transmission microscope was equipped with a LaB_6 electron source, operating at 120 kV, with an energy-dispersive *X*-ray (e.d.x.) detecting system as well as an electron energy loss spectrometer (Gatan 607).

E.d.x. analysis allowed the identification as well as the estimation of the concentrations of K, Cl, and Zn by the 'standardless ratio' technique using the Cliff–Lorimer equation[22] and the experimental k_{AB} values of Wood *et al.*[23] The 'thin film approximation' proved to be applicable to the thin film specimen.

E.e.l.s. analyses were performed in the transmission electron microscopy (t.e.m.) mode with diffraction coupling. In order to obtain a good signal-to-background ratio the collection angle was kept at 13.5 mrad by the objective aperture. *X*-Ray diffraction patterns of the powder samples employing Cu-K_α radiation were recorded with a Siemens one-circle diffractometer.

Results and Discussion

In order to prevent formation of artefacts, samples of zinc–graphite were prepared by reduction of fused zinc chloride with C_8K in anhydrous, argon-flushed thf under a stream of argon. For the investigations mentioned above each sample was quickly dispersed on an appropriate support and immediately placed into the sample chamber.

To obtain space-averaged structural information samples were subjected to *X*-ray diffraction. As a result four types of reflections, weak as well as strong, were recorded (Table 1), representing (*a*) reflections of graphite, (*b*) of KCl, (*c*) of metallic zinc,‡ and (*d*) several reflections caused by K_2ZnCl_4.[24] These peaks could well have been erroneously interpreted as being caused by intercalated zinc.[13,16,17] With the exception of the strong (002) reflections all other graphite reflections, because

---

* *Non-S.I. unit employed:* eV ≈ 1.60 × 10^{-19} J.

† Naturally occurring graphite was used for these investigations.

‡ The rather low *X*-ray diffraction peaks of zinc clearly demonstrate also the presence of larger particle sizes, unequivocally confirmed by a.e.m.

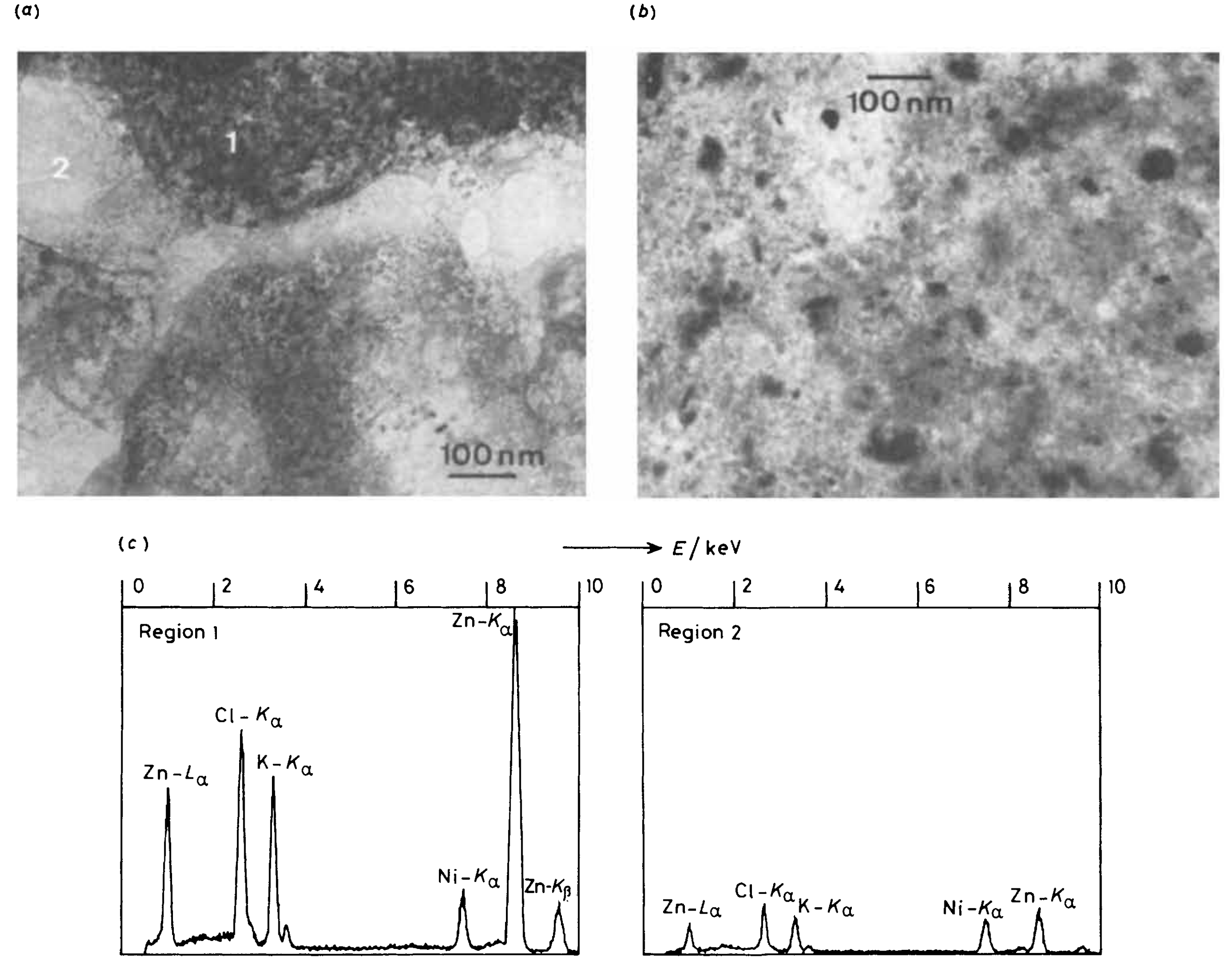

Figure 1. (*a*), (*b*) T.e.m. images showing finely dispersed zinc of different particle sizes on graphite. (*c*) E.d.x. spectra of regions 1 and 2, respectively, as marked

of texture effects, are weak. Since the (002) reflection is most indicative of unloaded graphite, and since all other reflections can be assigned to KCl, zinc, or K_2ZnCl_4, any zinc intercalated in graphite can be excluded.

Figure 1 depicts a typical bright-field image of graphite sheets not uniformly covered with particles of diameter 2—10 nm. While all the particles consist of the elements Zn, K, and Cl region 1 as compared to region 2 is particularly rich in Zn, as shown by e.d.x. analysis.

Additional information to disprove possible intercalation was obtained by selected area electron diffraction (s.a.e.d.) (Figure 2). Here the single point reflections arranged in circles are caused by graphite and the continuous circles by KCl. In addition there are rather diffuse reflection rings caused by highly dispersed metallic zinc of very low particle size, explaining its unprecedented high reactivity.[5,12,13] Figure 2 shows the (*hk*0) reflections of graphite sheets lying on the basal plane. Although the (001) reflections do not show in this orientation, in the case of intercalation there should be significant reflections besides those of (*hk*0) as found by the results of Evans and Thomas.[19] The complete absence of these reflections again disproves intercalation.

Figure 3 shows an electron energy loss spectrum, a suitable technique to detect elements below atomic number 11, which lacks the *K*-edge of oxygen, thus showing that the samples were not subject to deleterious atmospheric influences before or during instrumental analysis.

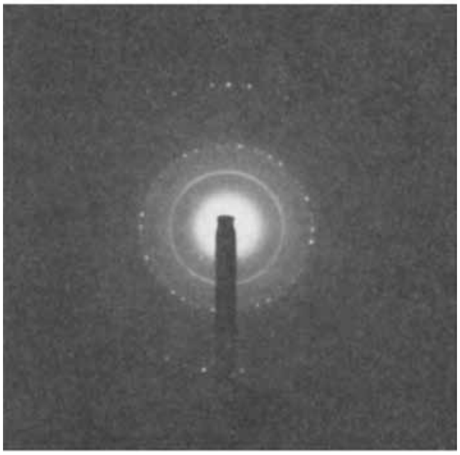

Figure 2. Electron diffraction pattern of zinc–graphite

Table 1. *X*-Ray diffraction data of zinc–graphite

$d_{obs.}$/nm	$I_{obs.}$	Phase
0.613	3	K_2ZnCl_4
0.509	8	K_2ZnCl_4
0.444	4	K_2ZnCl_4
0.358	8	K_2ZnCl_4
0.335	100	Graphite
0.315	80	KCl
0.2880	3	K_2ZnCl_4
0.2675	5	K_2ZnCl_4
0.2474	6	Zn
0.2308	4	Zn
0.2225	39	KCl
0.2090	17	Zn
0.2030	3	Graphite
0.1818	11	KCl
0.1686	5	Zn
0.1678	7	Graphite
0.1573	7	KCl

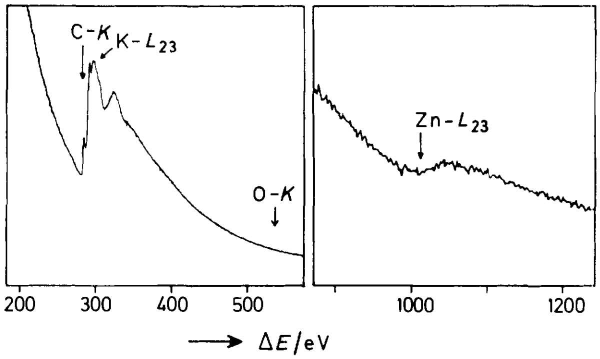

Figure 3. Electron energy loss spectrum (e.e.l.s.) demonstrating the absence of oxygen (*K*-edge) in the sample specimen of Figure 1

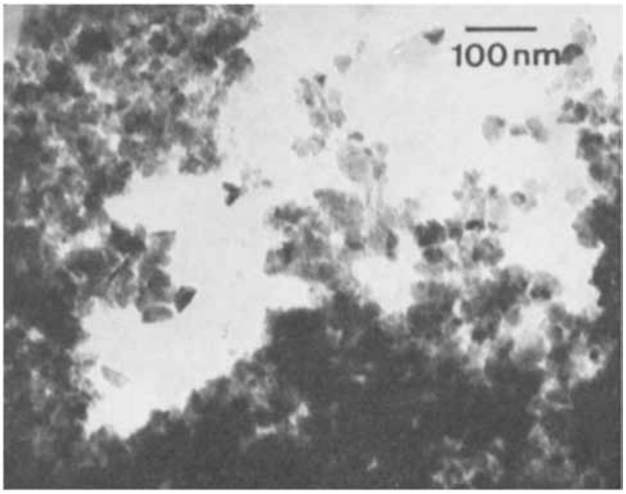

Figure 4. T.e.m. image of water-treated zinc–graphite showing ZnO on graphite

Table 2. *X*-Ray diffraction data of zinc–graphite after treatment with water

$d_{obs.}$/nm	$I_{obs.}$	Phase
0.335	100	Graphite
0.2818	7	ZnO
0.2600	5	ZnO
0.2473	8	ZnO
0.1914	2	ZnO
0.1675	5	Graphite
0.1622	2	ZnO
0.1573	3	ZnO

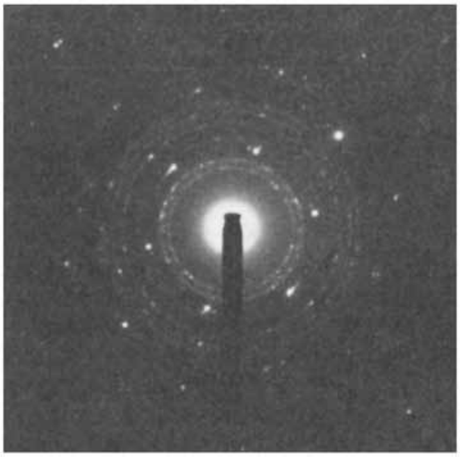

Figure 5. Electron diffraction pattern of water-treated zinc–graphite

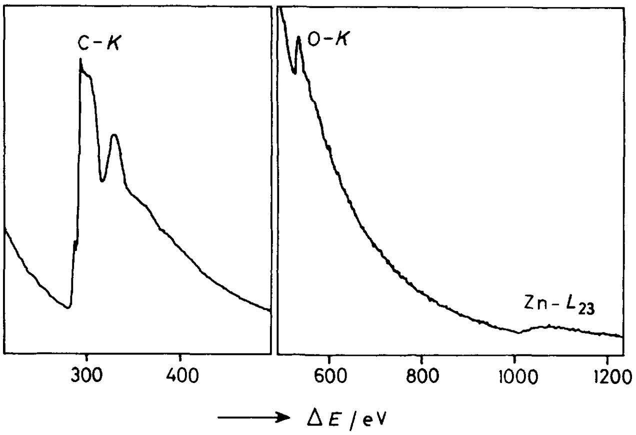

Figure 6. Electron energy loss spectrum of the particles shown in Figure 4

As demonstrated by *X*-ray diffraction (Table 2) and a detailed analysis of the particles in the bright-field image (Figure 4), water-treated zinc–graphite samples, contrary to previous assumptions,[13,16,17] consist of zinc oxide (zincite, 10—50 nm) on graphite only, as confirmed by e.e.l.s. and electron diffraction.

In summary, a.e.m. investigations of zinc–graphite comprising e.d.x., e.e.l.s., and s.a.e.d. conclusively demonstrate the presence of graphite in an unaltered condition, and merely acting as a support for KCl in admixture with finely dispersed metallic zinc. Both its undisturbed characteristic *X*-ray and electron diffraction patterns show no sign of intercalation of zinc. Certain parts of the *X*-ray spectrum were found to be potential sources of misinterpretations and could be unequivocally identified as reflections of K_2ZnCl_4.[24] The K_2ZnCl_4 also became clearly visible as large thin platelets in a.e.m., and the chemical composition was determined by quantitative e.d.x. analysis.

Acknowledgements

A. F. and H. W. gratefully acknowledge financial support by the Fonds zur Förderung der Wissenschaftlichen Forschung, Vienna. We also thank Dr. W. Geymayer for his encouragement and generous support of these investigations.

References

1 E. L. Muetterties, *Pure Appl. Chem.*, 1982, **54**, 83; J. Haber, *ibid.*, 1984, **56**, 1663.

2 A. Fürstner, *Oesterr. Chemiezeitschrift*, 1987, **88**, 30, 56.

3 A. Mendel, *J. Organomet. Chem.*, 1966, **6**, 97; G. Atnes, G. P. Chiusoli, and A. Marracchini, *ibid.*, 1973, **49**, 239.

4 A. A. P. Schreibmann, *Tetrahedron Lett.*, 1970, 4271; C. S. Chao, C. H. Cheng, and C. T. Chang, *J. Org. Chem.*, 1983, **48**, 4904; H. Kropf and J. Thiem, in 'Houben-Weyl—Methoden der Organischen Chemie,' ed. E. Müller, Thieme, Stuttgart, vol. 6/1b, 2.

5 R. Csuk, A. Fürstner, and H. Weidmann, *J. Chem. Soc., Chem. Commun.*, 1986, 775.

6 E. Santaniello and A. Manzocchi, *Synthesis*, 1977, 698; R. D. Clark and C. H. Heathcock, *J. Org. Chem.*, 1973, **38**, 3658.

7 P. Boudjouk, *Nachr. Chem. Tech.*, 1983, **31**, 798.

8 K. J. Klabunde, *Acc. Chem. Res.*, 1975, **8**, 393; 'Chemistry of Free Atoms and Particles,' Academic Press, New York, 1980.

9 R. D. Rieke, *Top. Curr. Chem.*, 1975, **59**, 1; *Acc. Chem. Res.*, 1977, **10**, 301.

10 D. Savoia, E. Tagliavini, C. Trombini, and A. Umani-Ronchi, *J. Org. Chem.*, 1980, **45**, 3227; H. Hart, B. Chen, and C. Peng, *Tetrahedron Lett.*, 1977, 3121; A. B. McEven, M. J. Guttieri, W. F. Maier, R. M. Laine, and Y. Shvo, *J. Org. Chem.*, 1983, **48**, 4436.

11 D. Savoia, C. Trombini, and A. Umani-Ronchi, *Pure Appl. Chem.*, 1985, **57**, 1887; R. Csuk, B. I. Glänzer, and A. Fürstner, *Adv. Organomet. Chem.*, 1988, **28**, 85.

12 R. Csuk, A. Fürstner, B. I. Glänzer, and H. Weidmann, *J. Chem. Soc., Chem. Commun.*, 1986, 1149; R. Csuk, A. Fürstner, H. Sterk, and H. Weidmann, *J. Carbohydr. Chem.*, 1986, **5**, 459; R. Csuk, A. Fürstner, B. I. Glänzer, V. Formacek, and H. Weidmann, *Carbohydr. Res.*, 1986, **157**, 235; A. Fürstner, *J. Organomet. Chem.*, 1987, **336**, C33.

13 G. P. Boldrini, D. Savoia, E. Tagliavini, C. Trombini, and A. Umani-Ronchi, *J. Org. Chem.*, 1983, **48**, 4108.

14 R. Csuk, A. Fürstner, and H. Weidmann, *J. Chem. Soc., Chem. Commun.*, 1986, 1802; A. Fürstner and H. Weidmann, *Synthesis*, 1987, 1071; A. Fürstner, R. Csuk, C. Rohrer, and H. Weidmann, *J. Chem. Soc., Perkin Trans. 1*, 1988, 1729.

15 For a review see, A. K. Holliday, G. Hughes, and S. M. Walker, 'Comprehensive Inorganic Chemistry,' ed. A. F. Trotman-Dickenson, Pergamon Press, Oxford, 1973, vol. 1, p. 1250; M. E. Volpin, Y. N. Novikov, N. D. Lapkina, V. I. Kasatochkin, Y. T. Struchkov, M. E. Kazakov, R. A. Stukan, V. A. Povitskij, Y. S. Karimov, and V. A. Zvarikina, *J. Am. Chem. Soc.*, 1975, **97**, 3366.

16 D. Braga, A. Ripamonti, D. Savoia, C. Trombini, and A. Umani-Ronchi, *J. Chem. Soc., Chem. Commun.*, 1978, 927; *J. Chem. Soc., Dalton Trans.*, 1979, 2026.

17 C. Ungurenasu and M. Palie, *Synth. React. Inorg. Metal-Org. Chem.*, 1977, **7**, 581.

18 H. Schäfer-Stahl, *J. Chem. Soc., Dalton Trans.*, 1981, 328; D. Braga, A. Ripamonti, D. Savoia, C. Trombini, and A. Umani-Ronchi, *ibid.*, 1981, 329.

19 E. L. Evans and J. M. Thomas, *J. Solid State Chem.*, 1975, **14**, 99.

20 D. J. Smith, R. M. Fischer, and L. A. Freeman, *J. Catal.*, 1981, **72**, 51.

21 E. Freund, J. Lynch, and R. Szymanski, *Ultramicroscopy*, 1986, **20**, 107; H. Dexpert, E. Freund, and J. Lynch, 'Quantitative Microanalysis with High Spatial Resolution,' The Metals Society, London, 1981, p. 101; J. J. Hren, J. I. Goldstein, and D. C. Joy (eds.), 'Introduction to Analytical Electron Microscopy,' Plenum Press, New York, London, 1979.

22 G. Cliff and G. W. Lorimer, *J. Microscopy*, 1975, **103**, 103.

23 J. E. Wood, D. B. Williams, and J. I. Goldstein, *J. Microscopy*, 1984, **133**, 225.

24 J. Watkins and R. Ashby, *Inorg. Chem.*, 1974, **13**, 2350.

Received 19*th February* 1987; *Paper* 7/314